eLIFE
elifesciences.org

Figures and figure supplements

Structure of a pore-blocking toxin in complex with a eukaryotic voltage-dependent K^+ channel

Anirban Banerjee, et al.

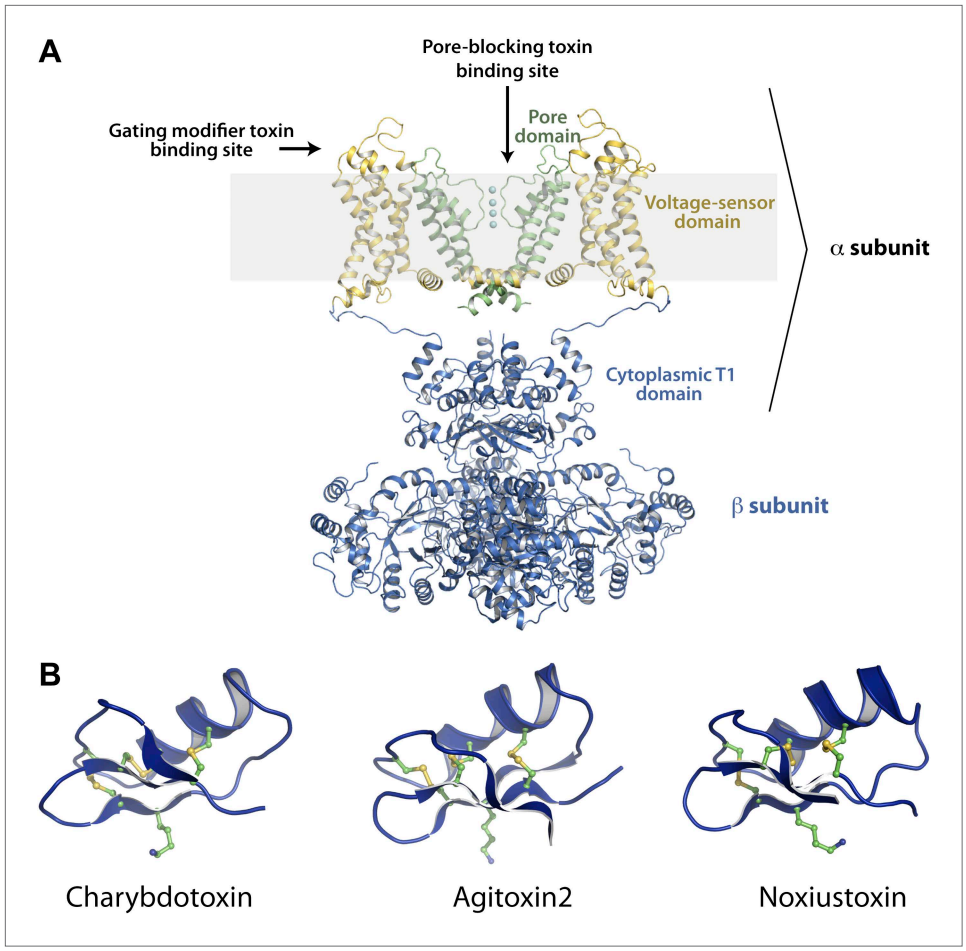

Figure 1. Structures of the channel used in this study and of representative scorpion toxins, including the one used in this study. (**A**) Side view showing two diagonal subunits of the paddle chimera channel in complex with the auxiliary β-subunit shown in ribbon trace (PDB ID 2R9R; ***Long et al., 2007***). The pore domain of paddle chimera is colored green, and the voltage sensor domain and the linker between the voltage sensor and the pore are colored in yellow. The cytoplasmic T1 domain and the auxiliary β-subunit are shown in blue. The K^+ ions in the selectivity filter are shown as cyan spheres. The area corresponding to the membrane is shaded in light gray. The channel forming α-subunit is indicated. Each α-subunit forms a complex with a β-subunit and four such α- and β-heterodimers make up the tetramer. Note that because the voltage sensors arrange around the pore domains in a domain-swapped fashion, the voltage sensor domains and the pore domains shown in the figure belong to different molecules of the tetrameric channel. Sites on the channel for binding the pore-blocking toxins and gating-modifier toxins are shown with arrows. (**B**) The lowest energy NMR structures of representative scorpion toxins with activity on K_v channels—charybdotoxin (CTX; PDB ID 2CRD; ***Bontems et al., 1991***), Agitoxin2 (AgTx2; PDB ID 1AGT; ***Krezel et al., 1995***) and Noxiustoxin (PDB ID 1SXM; ***Dauplais et al., 1995***) are shown in blue ribbon trace. A critical lysine (Lys27 for CTX and AgTx2 and Lys28 for Noxiustoxin) that is conserved in this family of toxins and the conserved cysteines are shown in ball and stick rendition and are colored by atoms.

DOI: 10.7554/eLife.00594.003

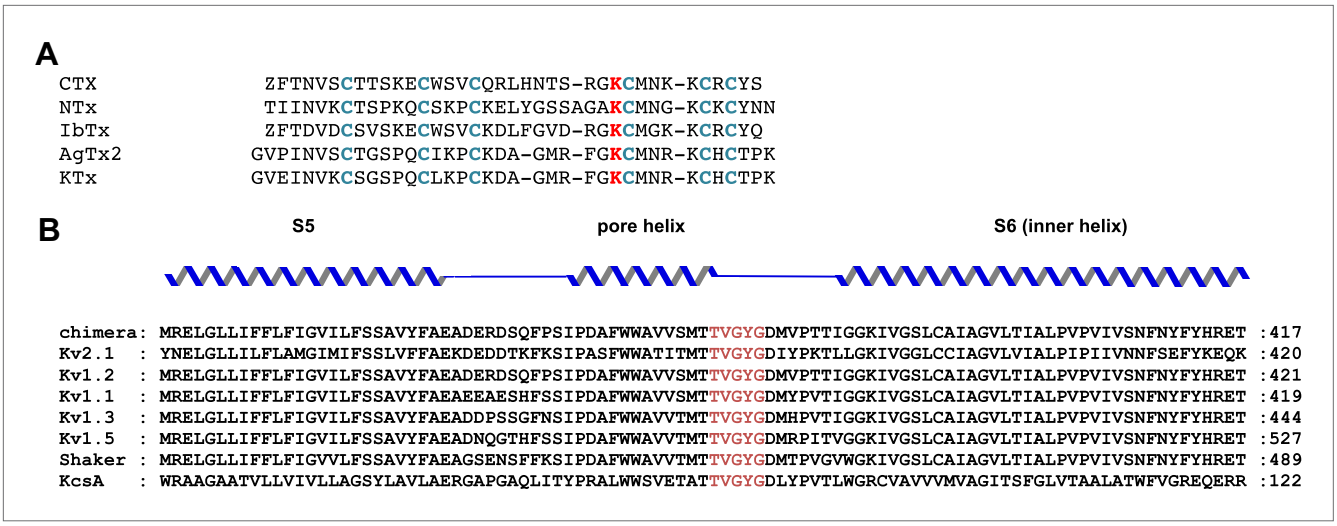

Figure 2. Sequence alignments of toxins and pore regions of K^+ channels. (**A**) Sequence alignments of five toxins belonging to the CTX family of K^+ channel toxins. The conserved cysteines that form disulfide bonds are shown in blue and the conserved lysine that competes with K^+ is shown in red. (**B**) Sequence alignment of the pore regions of selected members of the Shaker family of channels and KcsA–paddle chimera, rat K_v2.1 (GI:24418849), rat K_v1.2 (GI:1235594), human K_v1.1 (GI:119395748), human K_v 1.3 (GI:88758565), human K_v1.5 (GI:25952087), Shaker K_v (GI:13432103), and KcsA (GI:61226909). The sequence of the selectivity filter is shown in red.

DOI: 10.7554/eLife.00594.004

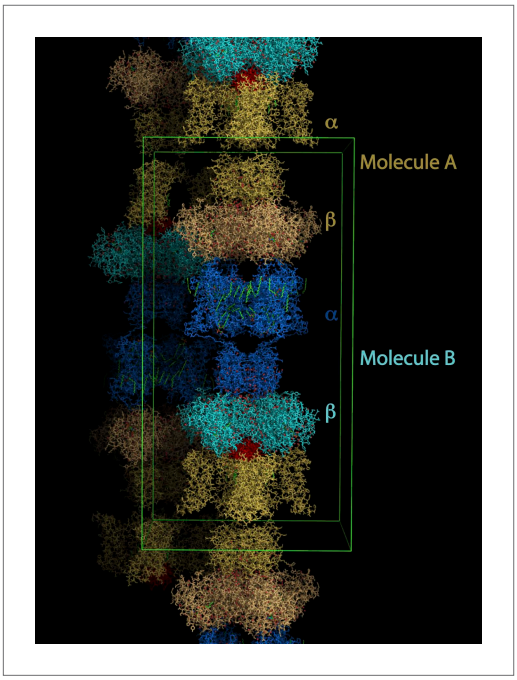

Figure 3. Lattice structure of paddle chimera–CTX complex. The asymmetric unit contains two independent molecules of channel forming α-subunits each in complex with an auxiliary β-subunit (see ***Figure 1A***). They are called molecule A, shown in stick rendition in different shades of cream; and molecule B, shown in stick rendition in different shades of blue. The toxin bound to molecule A was modeled and is shown in red. The outlines of a unit cell are shown in green.

DOI: 10.7554/eLife.00594.005

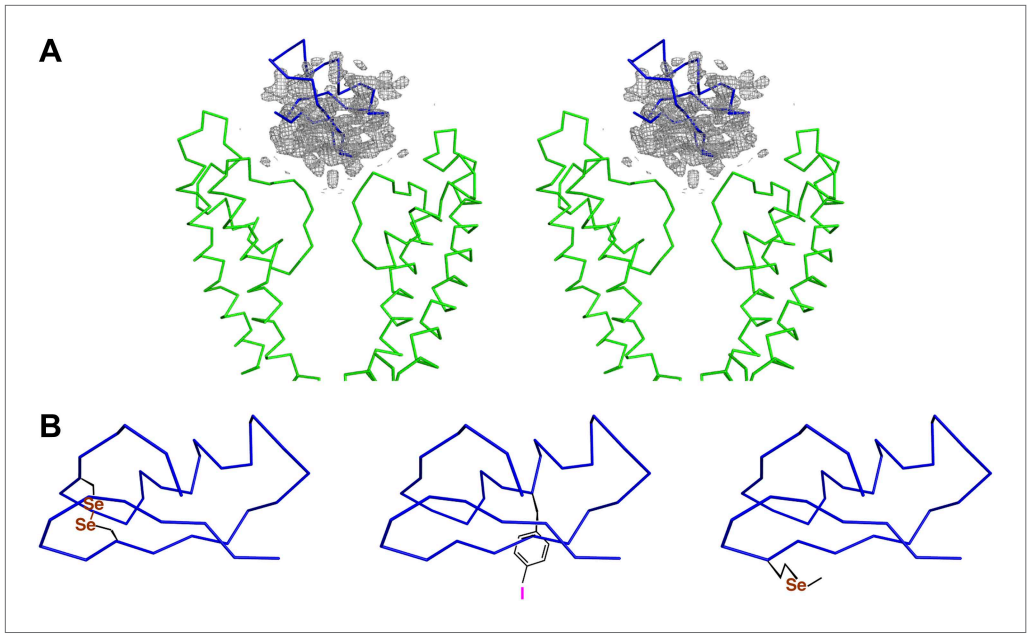

Figure 4. Initial placement of the CTX molecule in the toxin-channel complex and heavy atom derivatives used for subsequently improving the accuracy of placement. (**A**) Stereoview showing the pore domains from two diagonal subunits (molecule A) of paddle chimera (in the toxin-channel complex) in green α carbon trace and a toxin-omit weighted $2F_o - F_c$ electron density map in wire mesh at 0.8 σ contour level. The initial placement of the CTX molecule using the NMR structure (PDB ID 2CRD; ***Bontems et al., 1991***) is shown in blue α carbon trace within the omit map. (**B**) Chemical structures of the heavy atom derivatives of CTX used in this study are shown schematically. The NMR structure (PDB ID 2CRD; ***Bontems et al., 1991***) is used to depict the rest of the molecule in blue α carbon trace. The heavy atoms are shown in color, purple for iodine and copper for selenium.

DOI: 10.7554/eLife.00594.006

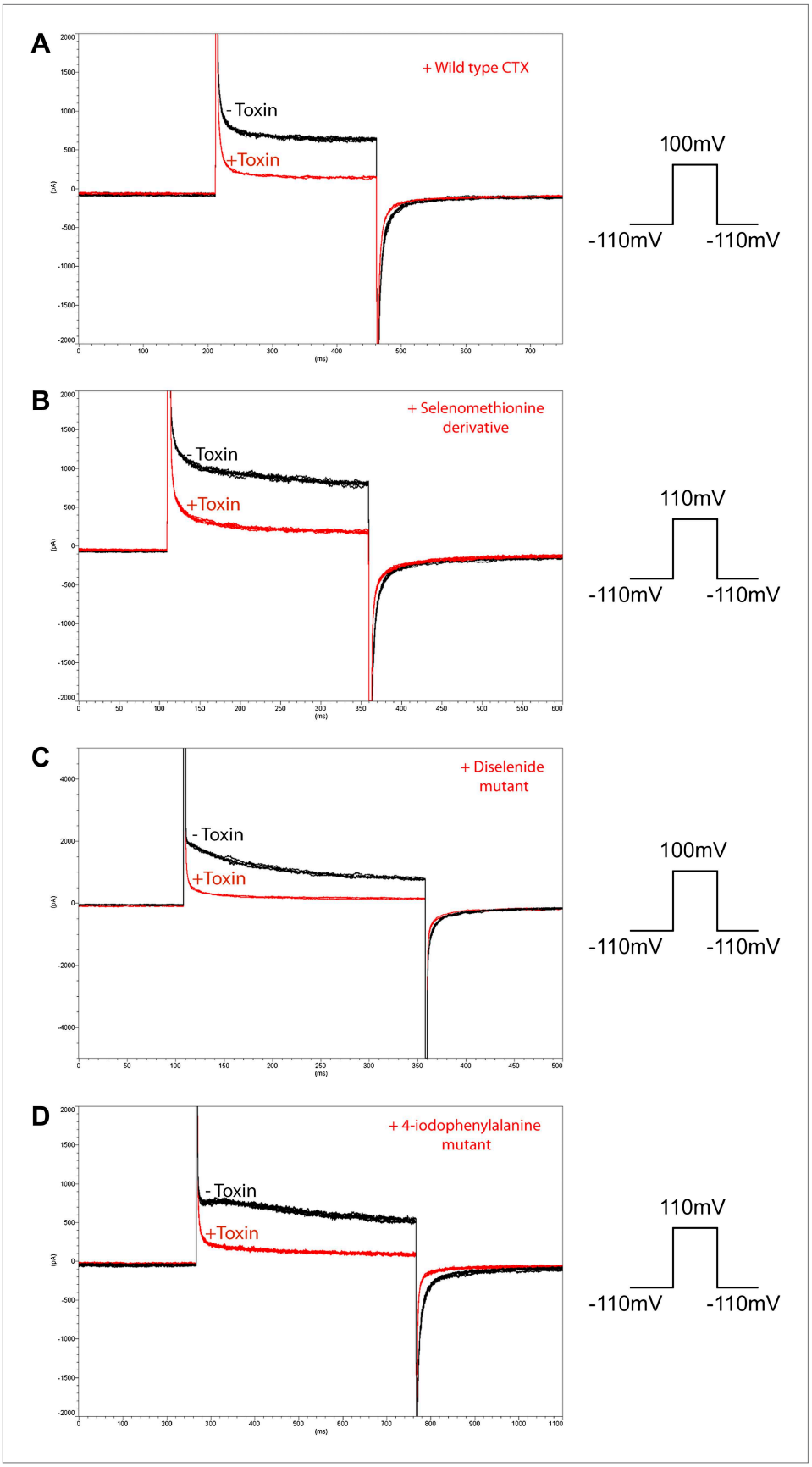

Figure 4—figure supplement 1. Continued on next page

Figure 4—figure supplement 1. Continued

Figure 4—figure supplement 1. Inhibition of paddle chimera by the different heavy atom derivatives of CTX used in this study. The experiments were carried out using a planar bilayer system (see 'Materials and methods'). The current traces before addition of the CTX derivative are shown in black, and the current traces after adding 100 nM CTX derivative are shown in red. Voltage pulses used are shown schematically on the right of each panel. (**A**) Wild-type CTX. (**B**) Selenomethionine derivative of CTX. (**C**) Diselenide mutant of Cys7-Cys28. (**D**) 4-Iodophenylalanine mutant of Tyr14.

DOI: 10.7554/eLife.00594.007

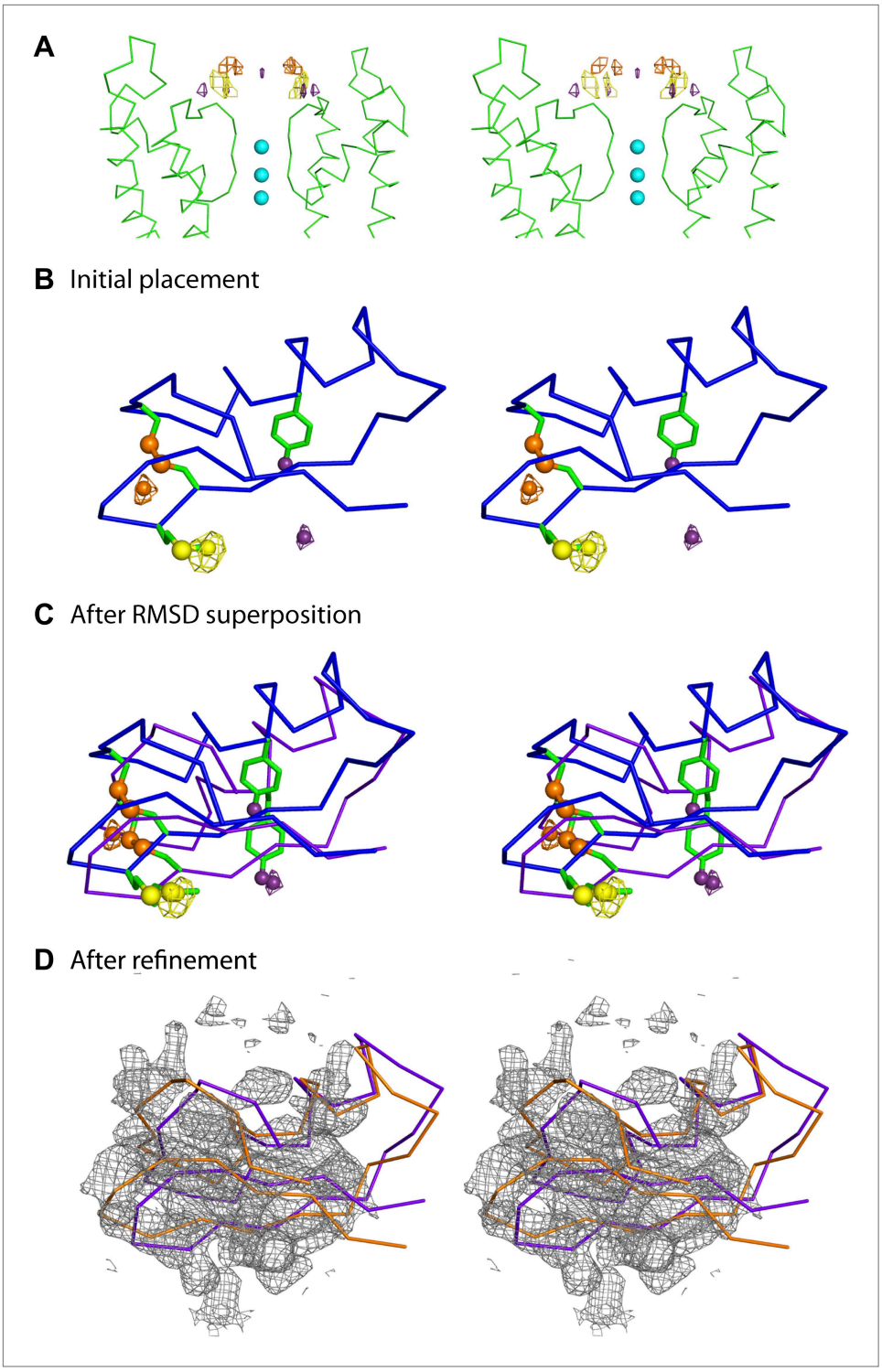

Figure 5. Improvement of the initial placement of the toxin. (**A**) Close-up stereoview showing part of the pore domains from two diagonal subunits (molecule A) of paddle chimera. Peak positions from the anomalous electron density maps for the three derivatives (see ***Figure 4B***) are shown and colored as follows—purple (4-iodophenylalanine mutant at position 14), orange (diselenide mutant of Cys7-Cys28), and yellow (SeMet mutant at position 29). Note that the four peaks correspond to the four positions of the toxin. In addition, the peak on the symmetry axis in the anomalous electron density map of the 4-iodophenylalanine mutant likely derives from reinforcement of noise peaks that are very close to the symmetry axis. (**B**) Stereoview showing initial placement of CTX in the omit

Figure 5. Continued on next page

Figure 5. Continued

map using the NMR structure (PDB ID 2CRD; ***Bontems et al., 1991***), in blue α carbon trace (same as in ***Figure 4A***). The heavy atoms in the depicted orientation are shown as oversized spheres with the corresponding peak positions (the closest of the four shown in ***Figure 5A***) in the anomalous electron density maps in wire mesh. Color-coding of the maps are the same as in ***Figure 5A***. A dummy atom has been placed to indicate the position of each peak. (**C**) The toxin molecule is shown in purple α carbon trace, after RMSD superposition of the heavy atom positions in the structure onto experimental peak positions as illustrated by the dummy atoms in ***Figure 5B***. The initial placement of the toxin as shown in ***Figure 5B*** is also shown in blue. (**D**) The final refined model of the toxin after crystallographic refinement (please see text and 'Materials and methods') is shown in orange α carbon trace together with the model after initial RMSD superposition in purple and a weighted $2F_o - F_c$ electron density map in wire mesh at 1σ contour level.

DOI: 10.7554/eLife.00594.008

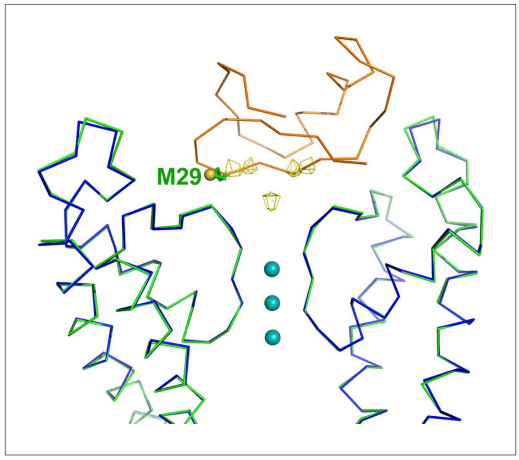

Figure 5—figure supplement 1. Validation of the model for the toxin. Shown is an RMSD superposition of molecule A with the bound CTX onto molecule B. The main chain atoms of the pore domains were used for the RMSD superposition. Shown are the pore domains (two diagonal subunits) from molecule A (in green), the pore domains (two diagonal subunits) from molecule B (in blue), and the CTX bound to molecule A in orange α carbon trace. The side chain of Met29 of CTX is shown in stick rendition, and the sulfur is shown as an oversized sphere. The peaks from the anomalous electron density map from the complex of the selenomethionine derivative of CTX with paddle chimera are shown in wire mesh. Note that the position of the sulfur is close to the expected position of selenium in the selenomethionine derivative of CTX. In addition to the four peaks corresponding to the four orientations of CTX, there is a peak on the fourfold symmetry axis, likely resulting from the reinforcement of noise in the electron density map.

DOI: 10.7554/eLife.00594.009

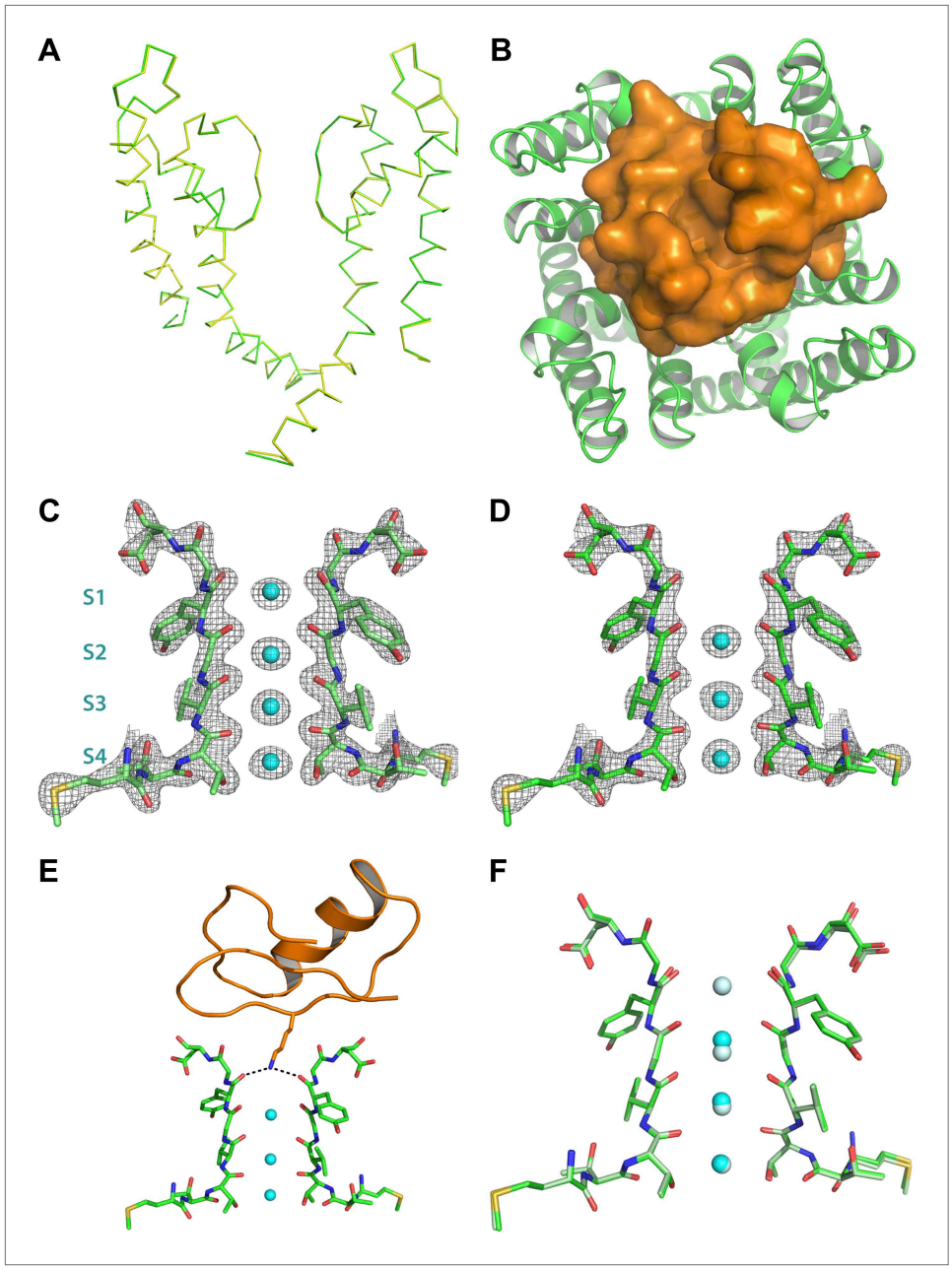

Figure 6. Structure of the toxin-channel complex. (**A**) Side view showing pore domains from two diagonal subunits from paddle chimera (yellow; PDB ID 2 R9R; ***Long et al., 2007***) and the toxin-channel complex (green) in α carbon trace. They have been superimposed by RMSD superposition of the main chain atoms from residues Met321-Thr414. (**B**) The tetrameric pore domain in the toxin-channel complex is shown in green ribbon trace from an extracellular view looking into the molecule. The bound CTX is shown in surface rendition in orange. (**C**) Side view of the selectivity filter (two diagonal subunits, molecule B) from the paddle chimera structure shown in stick rendition with the K^+ ions shown as cyan spheres. Sites S1 through S4 in the selectivity filter are labeled (labels on left side) in cyan. A weighted $2F_o - F_c$ electron density map contoured at 3σ is shown in wire mesh. (**D**) Side view of the selectivity filter (two diagonal subunits, molecule B) from the toxin-channel complex is shown in stick rendition with the K^+ ions shown as cyan spheres. A weighted $2F_o - F_c$ electron density map contoured at 3σ is shown in wire mesh. (**E**) The selectivity filter from the toxin-channel complex is shown in stick rendition with the K^+ ions shown as cyan spheres. Also shown is the bound CTX molecule in orange ribbon trace and the side chain of the Lys27 residue in stick rendition. Close contact between the amino headgroup and the carbonyl oxygen in the selectivity filter are shown in dotted lines. (**F**) RMSD superposed structures of the selectivity filter regions (same regions as

Figure 6. Continued on next page

Figure 6. Continued

shown in ***Figures 6C,D***) of the paddle chimera (pale green) and the toxin-channel complex (green) shown in stick rendition. The superposition was done using the main chain atoms from residues Met321-Thr414. The K^+ ions in the paddle chimera structure are shown in light blue and those in the toxin-channel complex in cyan.

DOI: 10.7554/eLife.00594.011

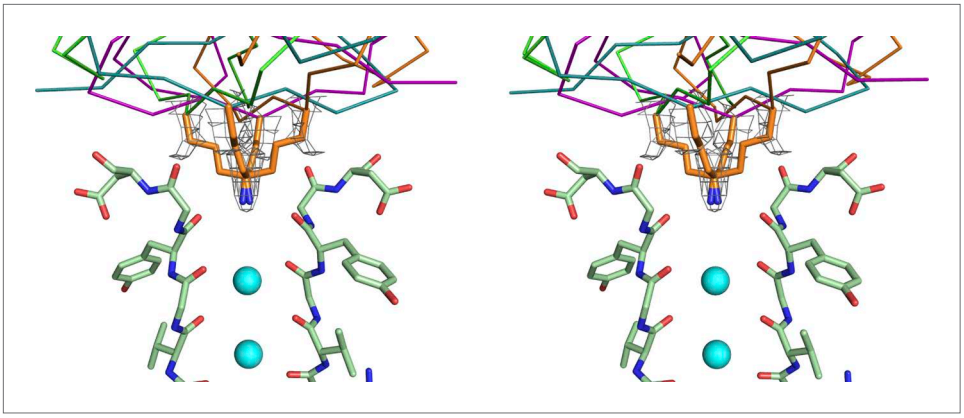

Figure 6—figure supplement 1. Electron density for the side chain of Lys27 of CTX in the paddle chimera–CTX complex. Shown in stereo is a close-up view of the top part of the selectivity filters of two diagonal subunits of paddle chimera in the paddle chimera–CTX complex (molecule A) in stick rendition. The K^+ ions in the selectivity filter are shown as cyan spheres. Also shown are the four symmetry-related orientations of the toxin molecule in purple, orange, teal, and green in α carbon traces. Only the lower parts of the toxin that are close to the channel are visible here. The side chains of Lys27 of CTX for the four corresponding orientations are shown in orange stick rendition. Also shown in wire mesh is a simulated annealing composite omit map at 1σ contour level, contoured on the atoms of the side chains of the four orientations of Lys27.

DOI: 10.7554/eLife.00594.012

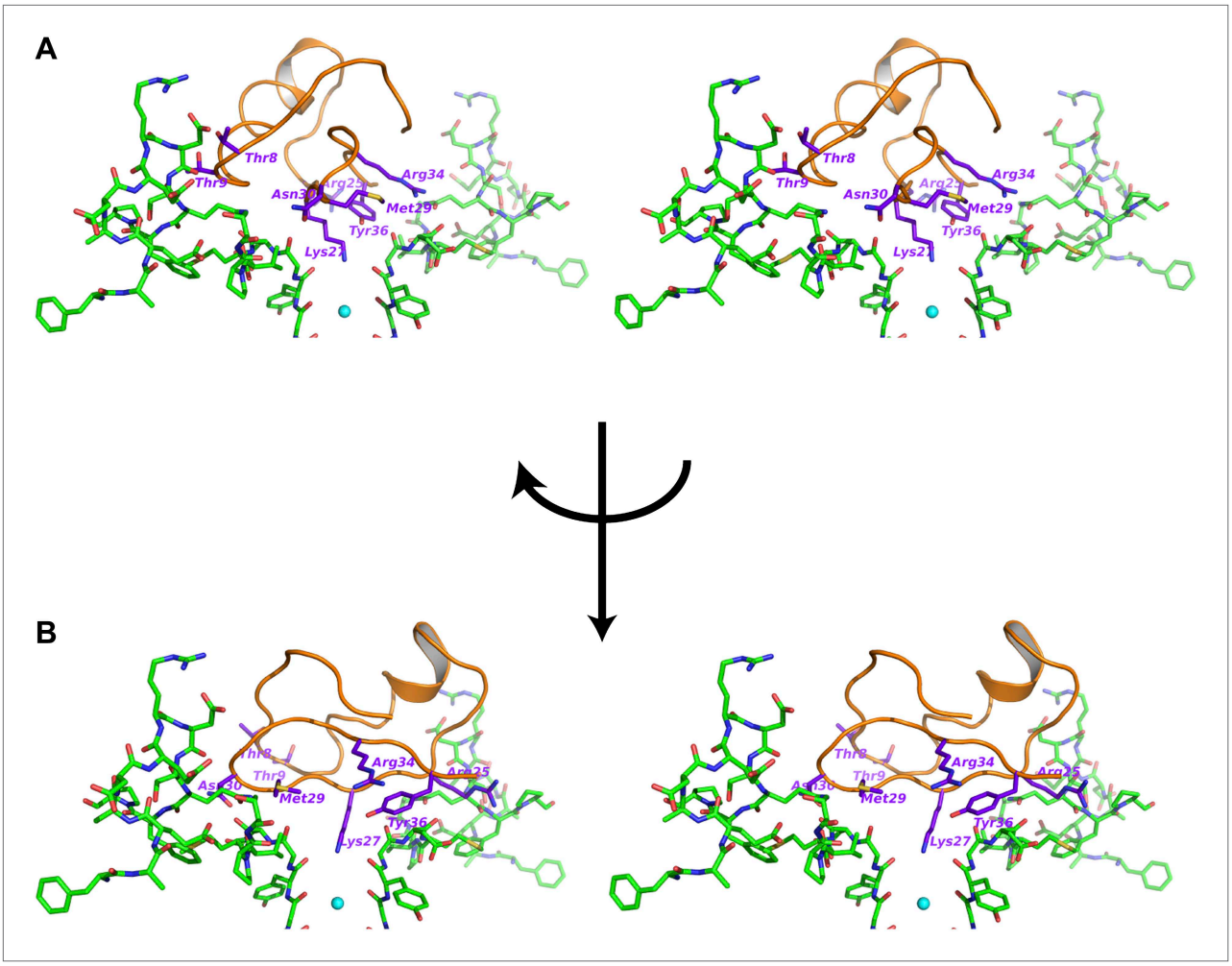

Figure 7. Interactions between the bound CTX and the channel. (**A**) Stereoview showing the CTX receptor region of paddle chimera from the toxin-channel complex shown in stick rendition together with the top parts of the selectivity filter. The bound CTX is shown in orange ribbon trace. Side chains of selected residues of the toxin are shown in purple and are labeled. (**B**) Shows a view orthogonal to that in (**A**). Consequently the receptor regions shown in (**B**) are from the two diagonal subunits of paddle chimera that are not shown in (**A**).

DOI: 10.7554/eLife.00594.013

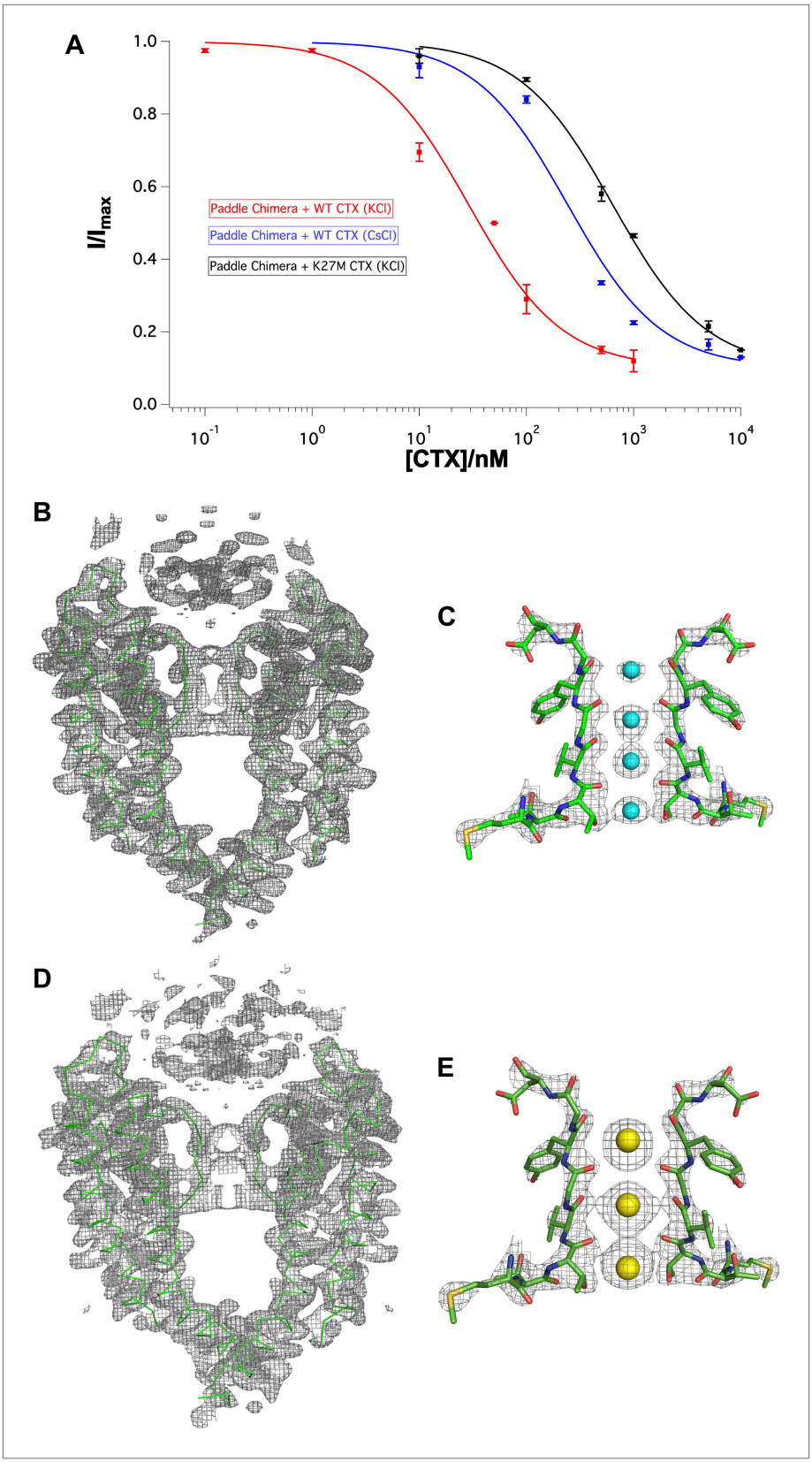

Figure 8. Effects of Lys27Met mutation of CTX and Cs^+ separately on toxin-channel interactions. (**A**) CTX inhibition. The fraction of unblocked current (I/Imax, mean ± SEM or range of mean; n = 2–4) is graphed as a function of CTX

Figure 8. Continued on next page

Figure 8. Continued

concentration (in nM) and fit to the equation I/Imax = 0.1 + 0.9 × (1 + [CTX]/K_d)$^{-1}$. Voltage pulses: holding −110 mV, depolarized to +110 mV, followed by a step back to −110 mV. Paddle chimera–wild-type CTX with KCl on both sides is shown in red, paddle chimera–wild-type CTX with CsCl on both sides is shown in blue and paddle chimera–Lys27Met CTX with KCl on both sides is shown in black. The modified equation accounts for approximately 10% current that is due largely to the channels facing the other side and are not blocked by toxin. (**B**) The pore domains from two diagonal subunits of paddle chimera (molecule A) in the Lys27MetCTX–paddle chimera complex are shown in green α carbon trace and a toxin-omit weighted $2F_o - F_c$ electron density map is shown in wire mesh at 1σ contour level. (**C**) Side view of the selectivity filter (two diagonal subunits; molecule B) of the Lys27Met CTX–paddle chimera complex shown in stick rendition with the K^+ ions shown as cyan spheres. An ion-omit weighted $2F_o - F_c$ electron density map is shown in wire mesh at 3.2σ contour level. (**D**) The pore domains from two diagonal subunits of paddle chimera (molecule A) in CTX–paddle chimera complex in CsCl, are shown in green α carbon trace and a toxin-omit weighted $2F_o - F_c$ electron density map is shown in wire mesh at 0.8σ contour level. (**E**) Side view of the selectivity filter (two diagonal subunits; molecule B) of the CTX–paddle chimera complex in CsCl shown in stick rendition with the Cs^+ ions shown as yellow spheres. A weighted $2F_o - F_c$ electron density map is shown in wire mesh at 3σ contour level.

DOI: 10.7554/eLife.00594.014

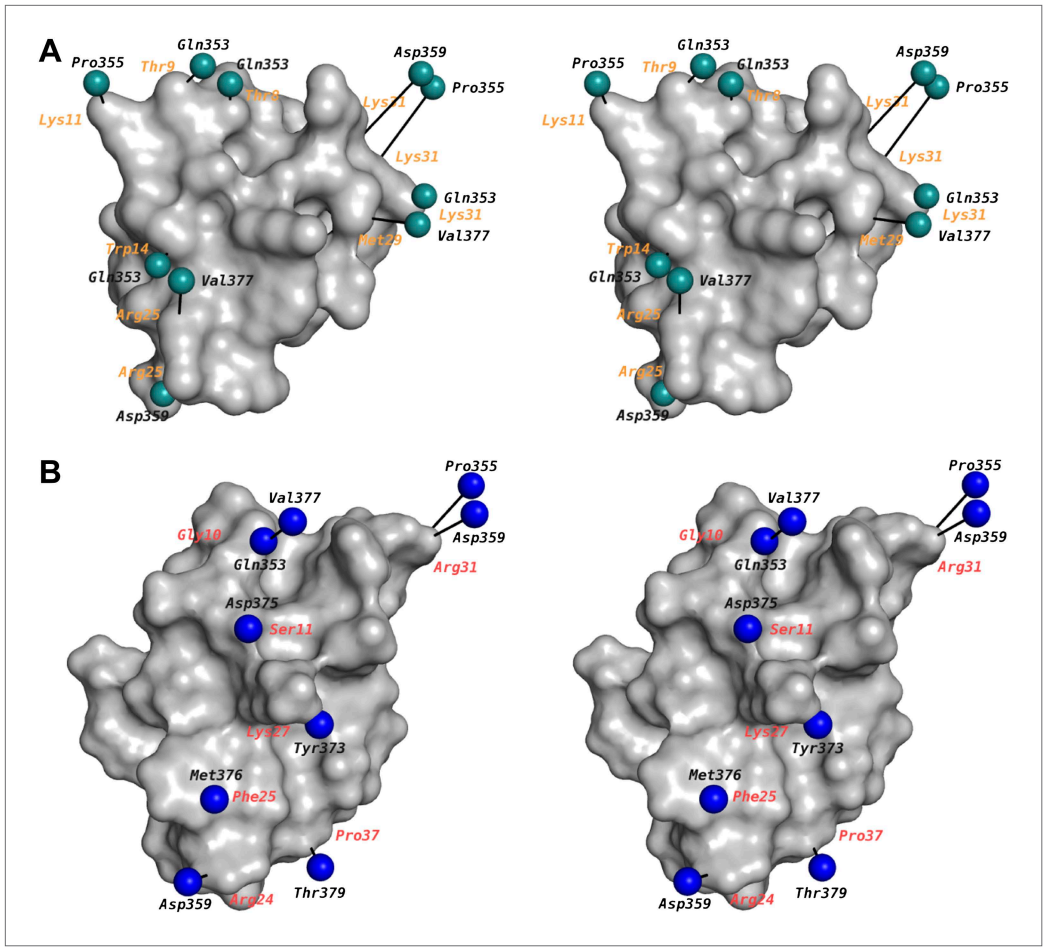

Figure 9. Mapping of toxin-channel interactions reported in literature on the structure of paddle chimera–CTX complex. (**A**) Shown is a stereoview of the bound CTX in surface rendition in the CTX–paddle chimera structure from an intracellular perspective viewing down the fourfold symmetry axis of the channel (channel not shown). Residues in the channel that have been reported in the literature to be proximal to the toxin are represented as green spheres taking the coordinates of the closest atom from the structure of the CTX–paddle chimera complex (see text). They are connected to the corresponding residues in the toxin with a black line. The corresponding residues in CTX are indicated in orange. Note that certain residues on the channel have been reported to be proximal to multiple residues on the toxin and thus they are represented more than once in the map. This figure shows data derived with CTX. (**B**) Shown are the residues in AgTx2 reported in the literature to be proximal to the channel, in the same format as (**A**). In order to depict AgTx2, it was superimposed on CTX in the paddle chimera–CTX complex using the published NMR structure of AgTx2 (PDB ID 1AGT; ***Krezel et al., 1995***) and using the guidelines in ***Krezel et al. (1995)***. AgTx2 is shown in surface rendition and the residues on the channel proximal to AgTx2 are shown as blue spheres. The corresponding residues in AgTx2 are indicated in red.

DOI: 10.7554/eLife.00594.015

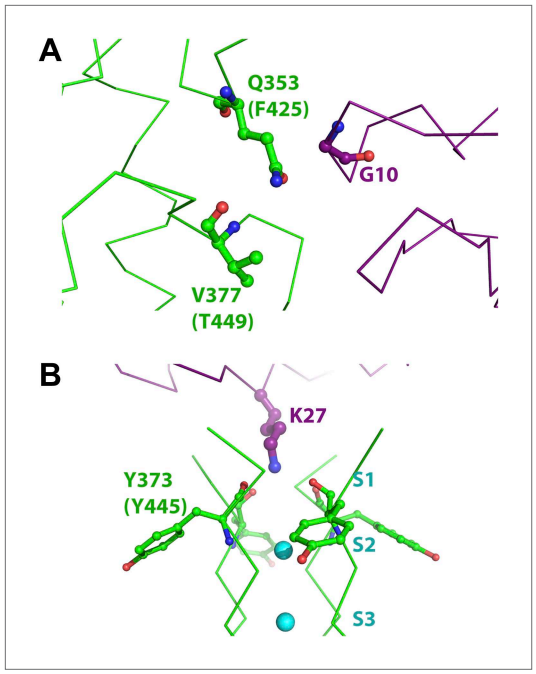

Figure 10. Mutant cycle data from ***Ranganathan et al. (1996)*** mapped onto the structure of paddle chimera–CTX complex. The toxin molecule shown in purple is AgTx2, which was superimposed onto CTX in the structure of the paddle chimera–CTX complex using the NMR structure of AgTx2 (PDB ID 1AGT; ***Krezel et al., 1995***). Guidelines in ***Krezel et al. (1995)*** were used for the superposition. (**A**) Close-up view of AgTx2 showing Glycine 10 in ball and stick rendition and the rest of the toxin in α carbon trace. The channel subunit that is most proximal to Gly10 is shown in green α carbon trace. Shown in ball and stick are residues Gln353 and Val377 in paddle chimera, that correspond to Phe425 and Thr449, respectively, in Shaker using a sequence alignment (***Figure 2B***). Ranganathan and MacKinnon reported that Gly10 is coupled to Phe425 and Thr449 in Shaker. (**B**) Close-up view of AgTx2 showing the side-chain of Lys27 in ball and stick rendition and the rest of the toxin in α carbon trace. The nearby regions of the selectivity filter from all four subunits of the channel are shown in green α carbon trace. Shown in ball and stick is Tyr373 in all four subunits of paddle chimera, which map onto Tyr445 in Shaker using a sequence alignment (***Figure 2B***). Ranganthan and MacKinnon reported Tyr445 to be coupled to Lys27, and this was dependent on the concentration of K^+.

DOI: 10.7554/eLife.00594.016